Adsorbate modification of the structural, electronic, and magnetic properties of ferromagnetic fcc {110} surfaces

D. S. D. Gunn and Stephen J. Jenkins

Department of Chemistry, University of Cambridge, Lensfield Road, Cambridge CB2 1EW, United Kingdom

(Received 8 July 2010; revised manuscript received 23 November 2010; published 3 March 2011)

We identify trends in structural, electronic, and magnetic modifications that occur on ferromagnetic {110} surfaces upon varying either the substrate material or the adsorbate species. First, we have modeled the adsorption of several first-row *p*-block elements on the surface of fcc Co{110} at two coverages [0.5 and 1.0 monolayer (ML)]. All adsorbates were found to expand the distance between the first and second substrate layers and to contract the distance between the second and third layers. The energetic location of a characteristic trough in the density-of-*d*-states difference plot correlates with the direction of the adsorbate magnetic coupling to the surface, and a trend of antiferromagnetic to ferromagnetic coupling to the surface was observed across the elements from boron to fluorine. A high fluorine adatom coverage (1.0 ML) was found to enhance the surface spin magnetic moment by ∼11%. Second, we also calculate and contrast adsorption of 0.5 and 1.0 ML of carbon, nitrogen, and oxygen adatoms on fcc iron, cobalt, and nickel {110} surfaces and compare the structural, electronic, and magnetic properties of these systems. Carbon and nitrogen are found to couple antiferromagnetically, and oxygen ferromagnetically, to all surfaces. It was found that antiferromagnetically coupled adsorbates retained their largest spin moment values on iron, whereas ferromagnetically coupled adsorbates possessed their lowest moments on this surface. The strongly localized influence of these adsorbates is clearly illustrated in partial density-of-states plots for the surface atoms.

DOI: 10.1103/PhysRevB.83.115403 PACS number(s): 71.15.Mb, 75.70.Rf, 75.50.Cc

I. INTRODUCTION

Iron, cobalt, and nickel are of interest to a wide range of industries, whether it be for their magnetoelectronic properties and use in recording media[1] or, particularly in the case of iron and cobalt, for their widespread use as Fischer-Tropsch catalysts.[2,3] Many of these applications, of course, are strongly sensitive to the *surface* properties of the material, which can differ somewhat from the bulk behavior due to the abrupt termination of both atomic and electronic structure at the vacuum interface. For example, narrowing of the *d*-band due to reduced coordination causes magnetic moments at these surfaces to be enhanced considerably from bulk values, and the relative significance of such surface-localized phenomena becomes potentially even greater when high-surface-area nanoparticles or ultrathin films are involved.

Surfaces are known to be highly sensitive to even small amounts of impurities, with adsorbates able to effect substantial reconstructions (e.g., oxygen on copper surfaces[4–7]) or to act as a surfactant when growing heterostructures (e.g., cobalt layers on copper[8–10]). The influence of such adsorbates is not merely limited to structural effects, however. Electronically, properties such as the work function are known to change upon adsorption,[11] while magnetically, several very interesting adsorbate-related effects have been observed; CO is known to induce a 90° switch in the easy axis of a Co/Cu{110} system,[12] and both the polarization of secondary electrons[13] and the coercive field[14] of cobalt-containing systems have been shown to alter drastically with the adsorption of a variety of adatoms. Adsorption on ferromagnetic systems has remained a popular topic of theoretical research over the last couple of decades, as the methods of describing such surfaces have improved, with the effect of adsorbates such as O,[15–19] N,[19–21] and CO[22–25] on iron of particular interest. Cobalt, too, has attracted a lot of attention with the adsorption of simple adatoms such as O, N, and C on Co{0001},[26–28] as well as the slightly more complex case of CO.[26,29,30] The fcc structure of cobalt, however, has been considerably less heavily investigated theoretically, with studies of O,[13,31] N,[13] and C[13] adsorption the most popular. Nickel, of course, is not left out, with a substantial quantity of literature looking at O,[32–34] CO,[35,36] NO,[37] and S[38] on various fcc surfaces.

Of particular interest is how adsorbates affect commercially important giant magnetoresistance (GMR) systems, such as those used in hard drives, with a view to both tailoring such devices by intentionally surface-doping them and to understanding what effect a mixture of residual gases would have on such systems when they are eventually exposed to the atmosphere. Ultrathin Co/Cu systems are merely one example of those that are GMR active,[39,40] yet a lot of experimental attention has been paid to it in the literature thanks to the relative ease of the epitaxial growth (where cobalt retains the fcc nature of the copper substrate, rather than its more common hcp structure).

Presented in this paper is a comprehensive theoretical comparison of the range of structural, electronic, and magnetic influences that a number of atomic adsorbates have on ferromagnetic {110} surfaces. First, we will investigate the trends that the first-row *p*-block elements exhibit in the modification of the fcc Co{110} surface's structural, electronic, and magnetic properties. The simple adatoms that have been chosen for investigation are hydrogen, boron, carbon, nitrogen, oxygen, and fluorine [at both 0.5 and 1.0 monolayer (ML) coverage]. Hydrogen, being a simple, common, atmospheric contaminant of surfaces, is also included to contrast the effect of the larger and more complex adatoms. Second, we investigate theoretically how three adsorbates, namely carbon, nitrogen, and oxygen, interact with surfaces of the three

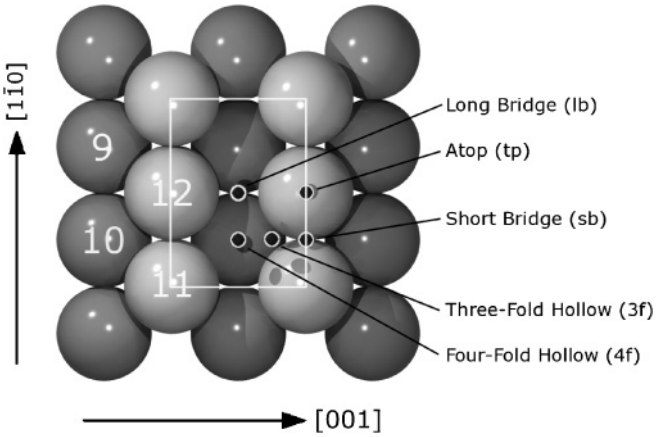

FIG. 1. High-symmetry adsorption sites and unit cell used for the Co{110} surface.

elemental itinerant ferromagnets—iron, cobalt, and nickel. To control for structural differences between different surfaces, we have studied adsorption on the fcc {110} facet only. This is certainly realistic for nickel, being a naturally fcc metal, and for cobalt and iron these fcc phases are important when considering epitaxial growth on substrates such as copper (for example as part of a multilayered structure for use in magnetoelectronic applications).[41] By focusing our study in this way, we hope to extract meaningful elemental trends in calculated properties as a function both of adsorbate and of substrate identity.

II. METHODOLOGY

The *ab initio* density functional theory (DFT) calculations in this work were performed using the CASTEP code.[43] The generalized gradient approximation (GGA) in the Perdew-Wang form,[44] ultrasoft pseudopotentials,[45] and a plane-wave cutoff of 340 eV were used throughout. Due to the ferromagnetic nature of the surfaces studied, the metal pseudopotentials include nonlinear core corrections (NLCCs) and the electronic spin is relaxed in all calculations. Atomic resolution of the spin magnetic moments was achieved via a Bader-type[46] topological analysis of the system.[47]

The supercell calculations consisted of six layers of metal[52] in a (2×1) unit cell with a minimum vacuum region of 12 Å. For cobalt, each adsorbate (H, B, C, N, O, F) was initially modeled in five high-symmetry sites (Fig. 1), at both 0.5 and 1.0 ML coverages. Adsorption of 0.5 and 1.0 ML of carbon, nitrogen, and oxygen adatoms on the iron and nickel surfaces was similarly modeled in the same high-symmetry sites (Fig. 1). Adsorption was allowed only on the top side of the cobalt slab, and the bottom four layers were held in an ideal bulk geometry.[53] The adsorbate, along with the top two layers of metal were allowed to relax according to the calculated forces. A $4 \times 6 \times 1$ **k**-point mesh[48] of similar density to that used in the trial bulk calculations was used for all surface calculations.

III. RESULTS AND DISCUSSION

A. Adsorbate trends on Co{110}

1. Structural characteristics and energetics

The adsorption energies, at each high-symmetry site, for the entirety of the adsorbates studied are shown in Table I, for both 0.5 and 1.0 ML coverages. The increase in energy seen as we raise the fractional coverage of hydrogen, nitrogen, oxygen, and fluorine implies that there is an enhanced repulsive interaction between the adsorbate adatoms. This is attributed to simple electrostatic repulsion between similarly charged species. At the higher coverage, boron moves to a higher coordination hollow site, and hydrogen, nitrogen, and fluorine remain in bridge sites. At 1.0 ML coverage the carbon adatoms become more embedded in the metal surface hollow sites, and Co atom 11 (see Fig. 1) is displaced by approximately 0.9 Å along the [001] direction, possibly indicating a nascent carbide-like structure.

Regardless of adsorbate, 0.5 ML coverage (in respective lowest-energy sites) results in an expansion between the first and second layers (i.e., the first interlayer spacing) of the cobalt surface, compared to the clean surface (Table II). Conversely, the second and third layers (the second interlayer spacing) are compressed to a larger extent than in the nonadsorbed system. Both of these effects are substantially amplified upon increased coverage (Table III).

Where the adsorbate does not change adsorption site upon increasing the fractional coverage (i.e., H, N, and F), we note that the vertical distance between the adsorbate and the surface, d_z, shortens considerably only in the case of N (from 0.24 to 0.05 Å). H and F remain at the same distance regardless of coverage. This seems to indicate that

TABLE I. Adsorption energies (eV) on the Co{110} surface. All adsorption energies refer to the overall change from the summed energies of the relaxed clean surface and either the respective gas-phase molecule (i.e., $X_{2(g)} \rightarrow 2X_{(a)}$; X = H, N, O, F) or atom (for boron and carbon). Values in bold indicate the lowest-energy adsorption site. Dashed values indicate where a stable adsorption geometry was not obtained.

	Adsorbate											
	H		B		C		N		O		F	
Site	0.5 ML	1.0 ML	0.5 ML	1.0 ML	0.5 ML	1.0 ML	0.5 ML	1.0 ML	0.5 ML	1.0 ML	0.5 ML	1.0 ML
TP	+0.42	+0.42	–	–	−5.90	–	–	+3.33	–	−1.18	−6.08	−5.23
SB	**−0.92**	**−0.87**	−4.62	−5.13	−7.12	−6.69	−0.04	+1.15	−4.78	−3.48	**−7.24**	**−6.33**
LB	−0.70	−0.60	**−6.12**	−5.86	**−8.44**	−8.04	**−1.82**	**−1.23**	−4.48	−4.21	−5.74	−5.49
3F	−0.86	−0.80	–	–	–	**−8.44**	−0.60	–	**−4.90**	−3.81	–	–
4F	−0.44	−0.35	−6.06	**−6.52**	−7.82	−8.38	–	+0.39	−3.96	**−4.45**	−5.64	−5.37

TABLE II. Structural characteristics upon 0.5 ML adsorption on the Co{110} surface. Parameters δ_{12} and δ_{23} are the average distances (normal to the surface) between layers 1 (the surface layer) and 2 and between layers 2 and 3, respectively, and d_z is the distance between the adatoms and the plane of the top-layer surface atoms. Distances are expressed as both an absolute value (Å) and as a percentage change relative to the equivalent distance in the clean surface.

		δ_{12}		δ_{23}		
Adsorbate	Site	(Å)	(%)	(Å)	(%)	d_z (Å)
H	SB	1.15	+4.54	1.30	−1.02	1.08
B	LB	1.16	+5.76	1.28	−2.08	0.51
C	LB	1.15	+4.96	1.31	−0.06	0.33
N	LB	1.21	+10.10	1.30	−0.90	0.24
O	3F	1.15	+4.95	1.29	−1.17	0.83
F	SB	1.20	+9.83	1.26	−3.85	1.45

increasing coverage of nitrogen strengthens the bond between the adsorbate and the surface, whereas higher concentrations of hydrogen and fluorine do not significantly alter the strength of the respective adsorbate-Co bond. At 0.5 ML coverages, N and F induce the largest expansion of the first interlayer spacing, increasing this separation by approximately +10% compared to the clean cobalt surface value. The remainder of the adsorbates all exhibit a slightly smaller (+5%–6%) expansive effect. Fluorine adsorption again has the largest impact (albeit compressive in this case) on the second and third layers (−4%), followed by boron (−2%), hydrogen, oxygen, and nitrogen (−1%), and finally carbon, which has a quite negligible influence on the second-to-third-layer distance.

Increasing the fractional coverage to 1.0 ML increases the expansion between the first and second cobalt layers by at least 150% compared to that induced by 0.5 ML coverage, and up to 1000% in the case of carbon (with the formation of a carbide-like structure). A similar increase is seen in the contraction of the distance between the second and third layers, with carbon again having the largest percentage increase over that seen at 0.5 ML coverage.

TABLE III. Structural characteristics upon 1.0 ML adsorption on the Co{110} surface. Parameters δ_{12} and δ_{23} are the average distances (normal to the surface) between layers 1 (the surface layer) and 2 and between layers 2 and 3, respectively, and d_z is the distance between the adatoms and the plane of the top-layer surface atoms. Distances are expressed as both an absolute value (Å) and as a percentage change relative to the equivalent distance in the clean surface.

		δ_{12}		δ_{23}		
Adsorbate	Site	(Å)	(%)	(Å)	(%)	d_z (Å)
H	SB	1.17	+7.09	1.28	−2.12	1.09
B	4F	1.44	+31.77	1.21	−7.28	0.45
C	3F	1.64	+49.79	1.20	−8.35	0.07
N	LB	1.38	+25.97	1.26	−3.97	0.05
O	4F	1.30	+18.61	1.23	−5.74	0.56
F	SB	1.28	+16.47	1.23	−5.74	1.46

2. Electronic and magnetic properties

The projected density of states (PDOS) plots for the surface layer of each adsorbate system are shown in Fig. 2 (for 0.5 ML coverage). For each adsorbate in Fig. 2, the average position of the *s* orbitals of the gas-phase atom/molecule are aligned with the lowest-energy *s* states in the adsorbed system. With the sole, obvious, exception of hydrogen, there is very little mixing of the adsorbate *s* states with the *d* states of the surface atoms. Instead, a significant proportion of the *d* states of the cobalt atoms are shifted to a lower energy when mixing with the *p* states of each adsorbate (again, excepting hydrogen). Upon adsorption, the spin-splitting of the adsorbate *p* states is greatly reduced and there is considerable broadening.

The densities of the surface-layer *d* states at the Fermi level remain relatively unchanged for the hydrogen, boron, oxygen, and fluorine adsorbed cases, in both majority and minority spin. In the cases of carbon and nitrogen adsorption there is only a very slight increase in the majority-spin states at the Fermi level, while the number of minority-spin states remains unchanged.

The percentage of majority-spin *d* states occupied in the clean surface is around 96.6%, with the minority occupation at 57.6%. Adsorption of the various elements naturally results in an alteration of the occupation of both the majority and minority spin to varying extents (Table IV). Also shown in this table are the calculated values of the *d*-band spin magnetic moment, $\mu_{d\,band}$, obtained by integrating the PDOS for the *d* orbitals alone. Broadly speaking, the surface-layer *d*-band polarization, P_d, follows the trend of the calculated values for the surface magnetic moment. P_d is defined in Eq. (1), where $n_\uparrow$ and $n_\downarrow$ are the numbers of surface-layer spin-up and -down *d* electrons, respectively:

$$P_d = \frac{n_\uparrow - n_\downarrow}{n_\uparrow + n_\downarrow}. \tag{1}$$

Boron, carbon, and nitrogen all reduce this polarization to around 0.186, through a combination of lowering majority occupation and increasing minority, and indeed, these three elements all reduce the surface-layer spin magnetic moment of the cobalt by a similar amount ($\sim 0.5\mu_B$). Oxygen does not alter the polarization significantly, and the surface spin moment value remains close to that of the clean surface. Fluorine, however, decreases the proportion of minority states occupied, and retains the same occupation for the majority, resulting in a higher polarization than for the clean surface. Consequently, we observe an enhanced surface spin moment for the cobalt atoms for this adsorbate.

Figure 3 shows the linear relationship that is present between the *d*-band spin magnetic moment and that for the full valence band using values from both the 0.5 and 1.0 ML coverage regimes. This implies that the counterpolarization of the *sp* electrons is proportional to the *d*-electron polarization, with the magnitude of the *sp*-band counterpolarization approximately 3% of the *d*-band polarization.

Even a superficial glance at the spin moments retained by the adsorbates (Table IV) highlights the broad relationship that an adsorbate that ferromagnetically couples to the surface

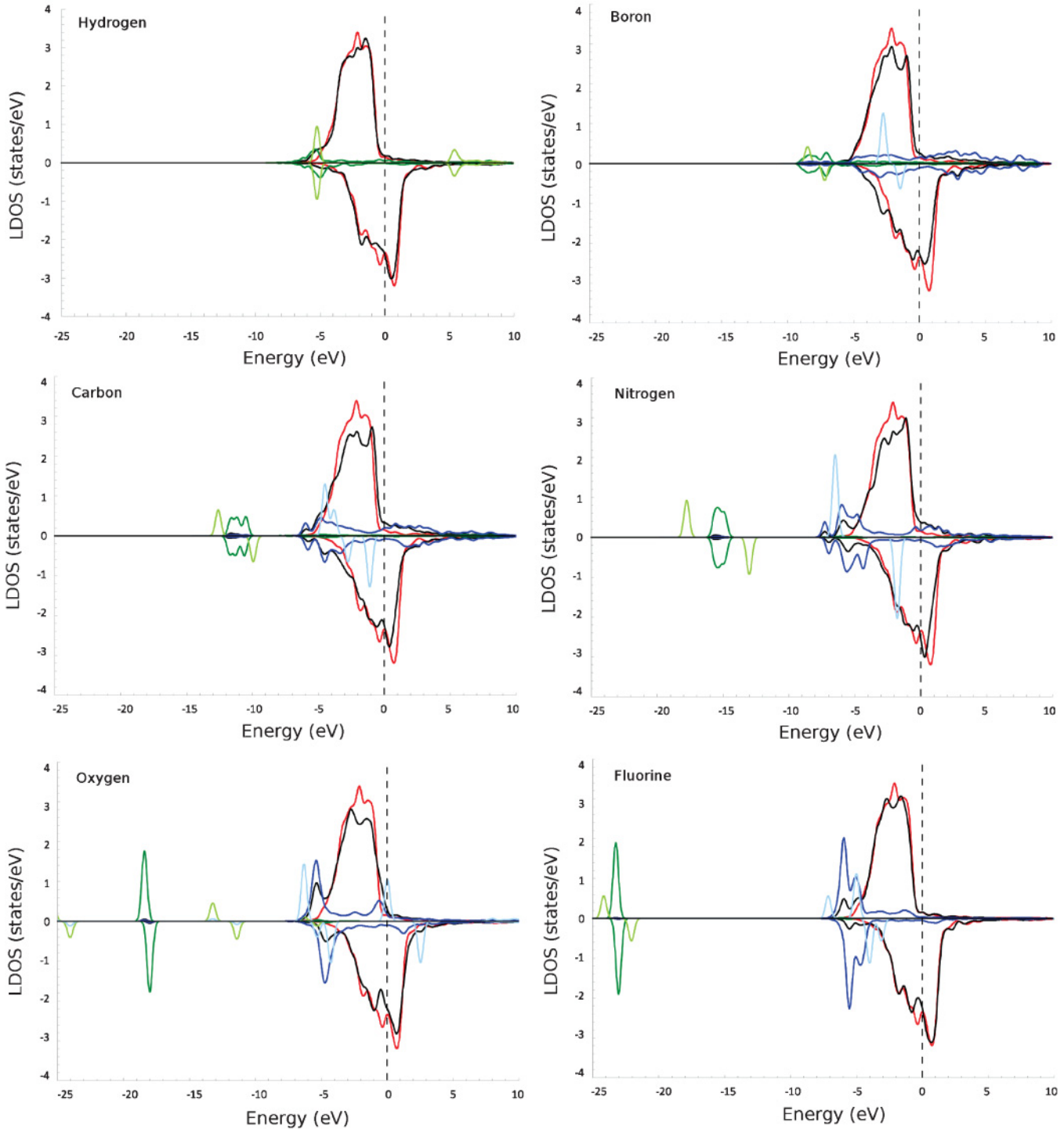

FIG. 2. (Color online) Spin-resolved projected density of states for the surface layer of various adsorbate-Co{110} systems at 0.5 ML coverage, with majority (minority) states on the upper (lower) half of each plot. The clean Co *d* states are shown in red, with the Co *d* states for the adsorbed surface shown in black with values averaged over all top-layer atoms. Adsorbate *p* states (dark blue) and *s* states (dark green) and gas-phase atomic (for boron and carbon) or molecular (for hydrogen, oxygen, nitrogen, and fluorine) *p* states (light blue) and *s* states (light green) are also illustrated. The Fermi level is calibrated to 0 eV and the gas-phase atomic and molecular states are calibrated to their adsorbed values, such that the average position of the lowest-energy *s* states are aligned.

(oxygen, fluorine) has either little effect on the surface spin moment or results in an enhancement. The magnitude of the spin moment on the adsorbate, however, does not appear to have any obvious correlation with the magnitude of the possible enhancement of the surface. Conversely, boron, carbon, and nitrogen all couple antiferromagnetically to the surface and all three result in a substantial decrease in the surface spin moment.

TABLE IV. Occupation and polarization (P_d) of the surface-layer d-band states and spin moments for the surface Co atoms and adsorbates at 0.5 ML coverage. Moments for the surface-layer d band ($\mu_{d\,band}$), surface-layer total ($\mu_{S\,layer}$), and adsorbate (μ_{Ads}) are in μ_B, and values for the surface layer are an average over all of the top-layer atoms.

X	Majority Occ. (%)	Minority Occ. (%)	P_d	$\mu_{d\,band}$	$\mu_{S\,layer}$	μ_{Ads}
	96.6	57.6	0.253	1.95	1.86	
H	95.5	58.7	0.239	1.84	1.76	0.00
B	92.6	63.5	0.186	1.46	1.40	−0.20
C	91.0	62.7	0.184	1.42	1.34	−0.15
N	91.5	62.7	0.187	1.44	1.41	−0.02
O	95.3	57.2	0.250	1.91	1.88	0.26
F	96.6	55.6	0.269	2.05	1.94	0.12

TABLE V. Occupation and polarization (P_d) of the d-band states and spin moments for the surface Co atoms and adsorbates at 1.0 ML coverage. Moments for the surface-layer d-band ($\mu_{d\,band}$), surface-layer total ($\mu_{S\,layer}$), and adsorbate (μ_{Ads}) are in μ_B, and values for the surface layer are an average over all of the top-layer atoms.

X	Majority Occ. (%)	Minority Occ. (%)	P_d	$\mu_{d\,band}$	$\mu_{S\,layer}$	μ_{Ads}
	96.6	57.6	0.253	1.95	1.86	
H	94.1	60.1	0.220	1.70	1.65	−0.01
B	88.9	66.5	0.144	1.12	1.06	−0.13
C	85.4	69.7	0.101	0.79	0.73	0.02
N	84.1	70.6	0.087	0.68	0.66	−0.05
O	92.0	58.6	0.222	1.67	1.68	0.20
F	96.6	53.7	0.285	2.15	2.06	0.18

The higher coverage regime paints a similar picture, as can be inferred from Appendix A (see Ref. 54) and Table V. Boron, carbon, nitrogen, and now oxygen all lower the d-band polarization, and all lower the surface magnetic moment by proportional amounts. Fluorine, meanwhile, increases the ratio again, and raises the surface magnetic moment of the cobalt to around $2.1\mu_B$, an increase of almost $0.3\mu_B$ over the clean-surface value.

The higher coverage does not appear to alter the densities of the surface-layer d-states at the Fermi level for either hydrogen or fluorine (Appendix A; see Ref. 54); however, now boron, carbon, nitrogen, and oxygen all show an increase in the number of majority states at the Fermi level, while the number of minority states remains unchanged.

A detailed study of the difference between the clean- and adsorbed-surface Co d states produces a similar picture for H, B, C, and N. Representative density-of-states difference plots can be seen in Figs. 4(a) and 4(b) for both majority and minority spin. For both 0.5 and 1.0 ML coverage, these aforementioned adsorbates exhibit similar patterns in their difference plots. First, for the majority-spin d states, we can see an increase in the density of states between −6 and −4 eV, coinciding with a high density of p states for the adsorbate (exact location alters with adsorbate). This region is followed by a broad decrease in the density of states (DOS), before rising rapidly to give a notable increase in the DOS sharply peaked just below the Fermi level. These features are interpreted as the bonding and antibonding combinations of the majority d states with the p states of the adsorbate (the two areas of increase in the DOS) and the region from which the states were previously located (the broad dip).

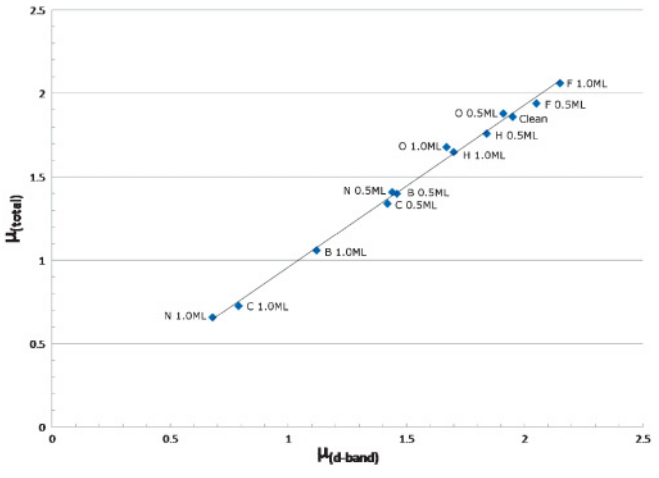

FIG. 3. (Color online) Graph illustrating the linear relationship between the average surface-layer d-band spin magnetic moment, $\mu_{d\,band}$, and the overall average value of spin magnetic moment per surface Co atom, μ_{total}. Values are shown in Tables IV and V.

This same motif is also present in the minority-spin case, albeit with the bonding and antibonding peaks less pronounced, and with much sharper and more individual troughs in the middle region. These features are shifted higher in energy compared to the majority-spin case and result in a distinct and deep trough in the DOS difference just *above* the Fermi level (for H, B, C, and N). This latter feature appears to be a good indicator of how the adsorbate influences the surface spin moment of the cobalt. For the three systems where an *increase* in moment is observed—0.5 ML O coverage and both 0.5 and 1.0 ML F coverage—this trough is located just *below* the Fermi energy [Fig. 4(d)]. Such a correlation makes perfect sense, since removal of minority d states from *below* the Fermi level should tend to drive the surface moment up, while removal of these states from *above* the the Fermi level would have no influence; the changes in majority-spin d states tend always to *reduce* the surface moment. It would be intriguing to determine whether this clear spectroscopic signature can be observed in spin-polarized photoemission experiments.

Following topological analysis, layer-resolved charges and spin moments are shown in Tables VI and VII, respectively. Regardless of the adsorbate, electrons are transferred primarily from the surface layer to the adatom (see Fig. 5). As the fractional coverage of the adsorbate is increased, the magnitude of the (negative) charge transferred to each adsorbate atom decreases while that withdrawn from the surface layer increases. The exception to this is with boron, where the charge transferred to the adsorbate increases with coverage. A basic interpretation of electronegativities would lead us to expect that fluorine would incur the greatest charge transfer to the adsorbate, followed by oxygen, nitrogen, carbon, etc.

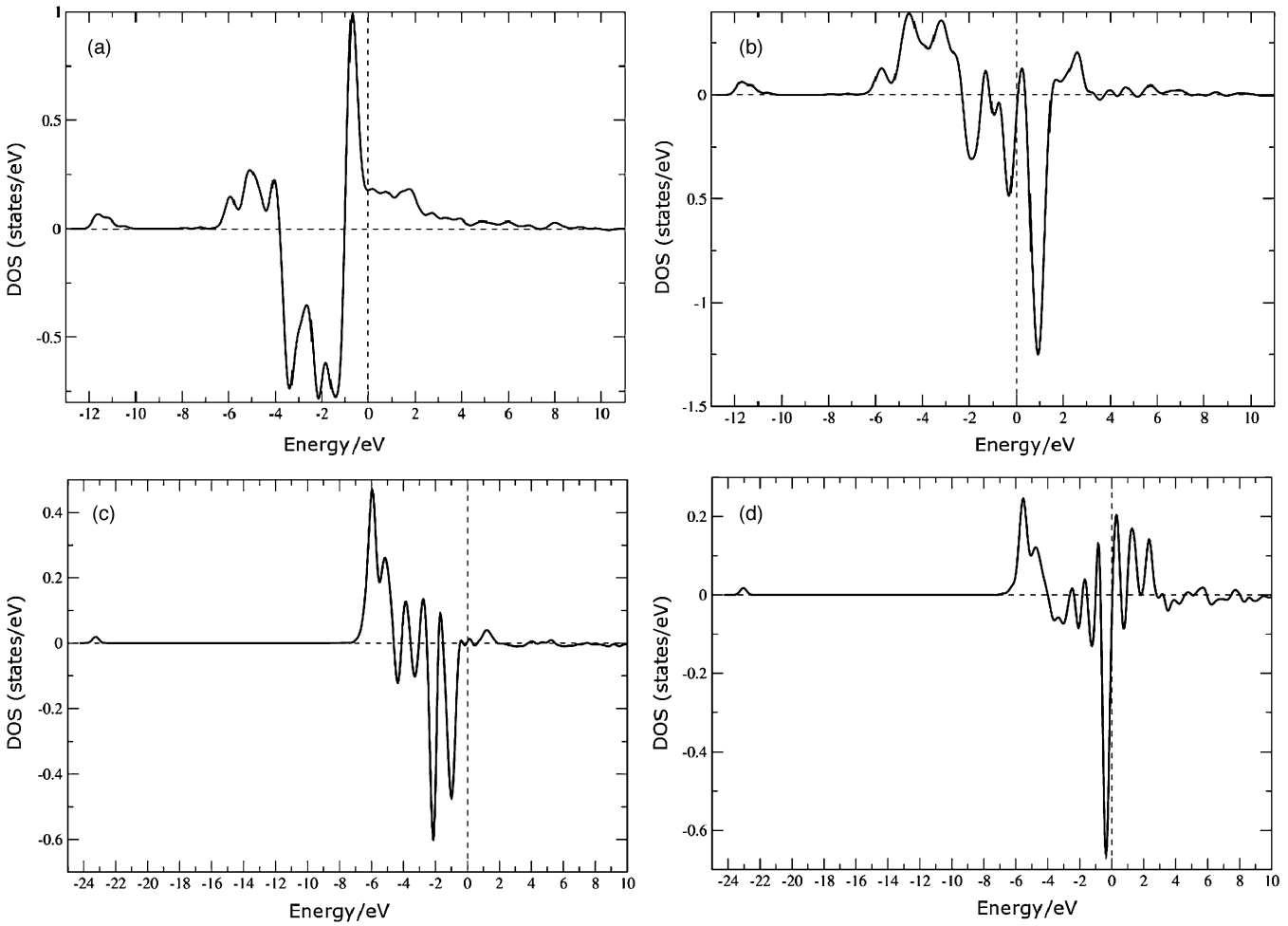

FIG. 4. Difference plots between the surface-layer *d* states of the cobalt in 0.5 ML adsorbate-covered systems and that for the clean surface. The Fermi level is marked at 0 eV. Panels (a) and (b) represent the changes that occur in the majority and minority spin of the carbon-covered system, respectively (this being essentially representative of the changes that occur upon adsorption of H, B, C, and N). Panels (c) and (d) represent changes that occur in the majority and minority spin of the fluorine-covered system, respectively.

However, we observe that this is not in fact the case, with the charge on nitrogen instead being the greatest. These results indicate that depolarization of adsorbates generally becomes important at high coverage and that the charging of subsurface layers cannot be ignored.

Looking at the spin magnetic moments retained by the adsorbates [Table VII and Figs. 6(a) and 6(b)], some interesting trends emerge. Carbon is found to couple antiferromagnetically to the cobalt surface (at 0.5 ML coverage, with essentially no spin coupling at 1.0 ML), nitrogen only retains a weak antiferromagnetic (AF) coupling, and oxygen exhibits a ferromagnetic (FM) relationship with the surface. Extending this trend further along the periodic table, we see that boron has a stronger AF coupling than carbon, but fluorine shows a weaker FM coupling than oxygen. We can suggest, therefore, that the FM nature of the bond between an adsorbate and this cobalt surface increases to a peak at oxygen, from both directions. The strength of the FM (or AF) coupling between the adsorbate and the surface is, however, not a direct measure of the surface moment of the cobalt. Even though fluorine

TABLE VI. Layer-averaged net atomic charge values (in e) for the adsorbate (Ads), surface (S), and first subsurface (S-1) layers.

	Adsorbate system												
		H		B		C		N		O		F	
	Clean	0.5 ML	1.0 ML	0.5 ML	1.0 ML	0.5 ML	1.0 ML	0.5 ML	1.0 ML	0.5 ML	1.0 ML	0.5 ML	1.0 ML
Ads		−0.36	−0.30	−0.23	−0.31	−0.85	−0.48	−1.10	−0.97	−1.01	−0.98	−0.72	−0.62
S	0.01	0.17	0.25	0.07	0.27	0.28	0.61	0.33	0.57	0.36	0.70	0.32	0.55
S-1	−0.03	0.00	0.04	0.04	0.04	0.12	−0.12	0.18	0.39	0.11	0.24	−0.01	0.05

TABLE VII. Layer-averaged net atomic spin moment values (in μ_B) for the adsorbate (Ads), surface (S), and first subsurface (S-1) layers.

	Adsorbate system											
		H		B		C		N		O		F	
	Clean	0.5 ML	1.0 ML	0.5 ML	1.0 ML	0.5 ML	1.0 ML	0.5 ML	1.0 ML	0.5 ML	1.0 ML	0.5 ML	1.0 ML
Ads		0.00	−0.01	−0.20	−0.13	−0.15	0.02	−0.02	−0.05	0.26	0.20	0.12	0.18
S	1.86	1.76	1.65	1.40	1.06	1.34	0.73	1.41	0.66	1.88	1.68	1.94	2.06
S-1	1.63	1.69	1.75	1.42	1.32	1.31	1.52	1.50	1.11	1.75	1.65	1.71	1.76

exhibits a weaker FM coupling compared to oxygen, the cobalt surface moment induced by the adsorbate is greater than that for oxygen. Similarly, nitrogen's weak AF coupling still incurs a suppression of the surface cobalt spin moment to the same extent seen for boron at 0.5 ML coverage and to an even greater extent at 1.0 ML coverage.

The results presented here for carbon, nitrogen, and oxygen broadly agree with our similar work on iron and nickel surfaces (presented in the following section), where carbon and nitrogen are found to depress the spin moment of the surface layers. Interestingly, the lower (0.5 ML) coverage of oxygen was also found to depress the surface magnetic moment on iron and nickel, in contrast to the slight enhancement seen here in the case of Co{110}. Our results are also in accord with previous results of adsorption on the hcp Co{0001} surface.[28] In their work, Pick and Dreyssé reported that a low coverage of carbon and nitrogen show a more marked suppression of the cobalt surface spin moment, compared to that caused by oxygen. At a higher coverage, they found that oxygen suppresses the surface moment to a similar degree as carbon. They did also find, however, that this suppressive effect for oxygen was geometry dependent—particularly on the O-Co distance (in the direction perpendicular to the surface), which was fixed at either (1.9 or 2.0 Å) in their calculations, rather than being allowed to relax, as is the case here. Nevertheless, we also find that at 0.5 ML coverage carbon and nitrogen suppress the surface spin magnetic moment of cobalt by a larger amount than oxygen. Furthermore, we also find that at higher coverage oxygen does indeed suppress the surface moment, although not quite to the extent that carbon does.

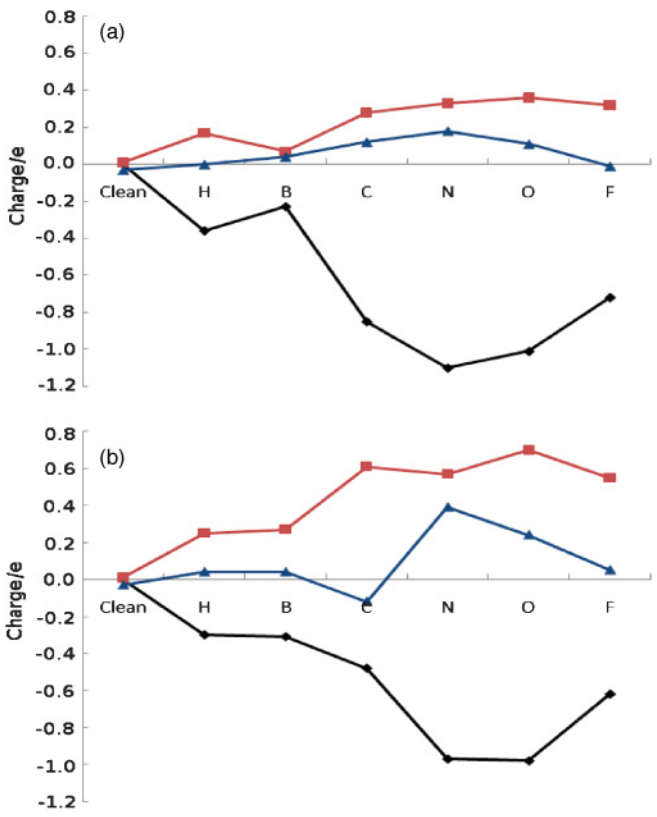

FIG. 5. (Color online) Layer-averaged net atomic charge values for the adsorbate (black line with diamonds), surface (red line with squares), and subsurface (blue line with triangles) layers, at both 0.50 ML (a) and 1.0 ML (b) coverage. Values are shown in Table VI.

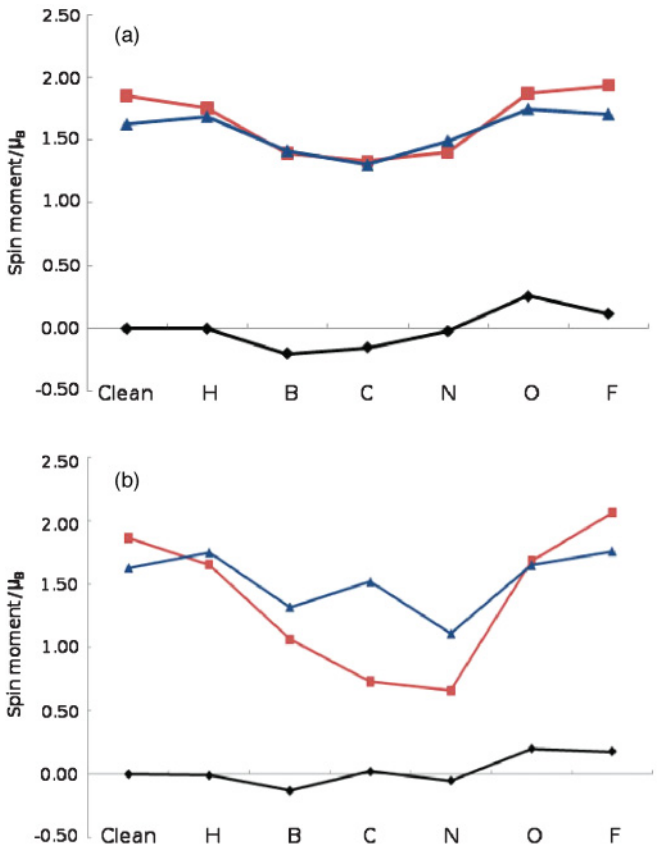

FIG. 6. (Color online) Layer-averaged net atomic spin moment values for the adsorbate (black line with diamonds), surface (red line with squares), and subsurface (blue line with triangles) layers, at both 0.50 ML (a) and 1.0 ML (b) coverage. Values are shown in Table VII.

TABLE VIII. Adsorption energies (eV) on the fcc Fe{110} surface. All adsorption energies refer to the overall change from the summed energies of the relaxed clean surface and the respective gas-phase molecule (i.e., $X_{2(g)} \rightarrow 2X_{(a)}$; $X = \mathrm{N}$, O) or atom (for carbon). Values in bold indicate the lowest-energy site. Dashed values indicate highly unstable sites, where convergence was not obtained.

	Adsorbate					
	C		N		O	
Site	0.5 ML	1.0 ML	0.5 ML	1.0 ML	0.5 ML	1.0 ML
TP	−7.63	−7.48	−1.70	+1.86	−3.74	−2.63
SB	−7.59	−7.22	−1.62	−0.75	−5.80	−4.85
LB	**−9.18**	**−8.77**	**−3.84**	**−3.31**	−6.12	−5.92
3F	–	–	−2.42	−1.84	**−6.24**	−5.51
4F	−8.62	−8.29	−1.80	−1.84	−5.14	**−6.15**

B. Substrate trends probed with carbon, nitrogen, and oxygen

1. Structural characteristics and energetics

Adsorption energies for carbon, nitrogen, and oxygen on each surface are shown in Table VIII for iron, Table IX for cobalt, and Table X for nickel. Several sites were found to be inherently unstable and resulted in the adsorbate migrating to a different location. In these instances we have simply marked their adsorption energy in the appropriate table with a "—".

The structural changes upon adsorption in the most stable position are shown for iron (Table XI), cobalt (Table XII), and nickel (Table XIII).

For iron, we note that the long-bridge site is the one that is preferred for carbon and nitrogen, and that these adsorbates induce similar structural effects on the surface at their respective 0.5 and 1.0 ML coverages. At 0.5 ML coverage, these two adsorbates both cause a moderate contraction of the top two surface layers (∼0.05 Å) and a smaller contraction (∼0.02 Å) between the second and third surface layers. At the higher, 1.0 ML, coverage, both carbon and nitrogen now cause an expansion in the top two layers of iron (∼0.04 Å) and a stronger contraction in the second and third layers (∼0.08 Å). While increasing the coverage of carbon and nitrogen to 1.0 ML results in the adatoms lying flatter on the surface (reduced d_z), the X-S and X-(S-1) distances remain

TABLE IX. Adsorption energies (eV) on the fcc Co{110} surface. All adsorption energies refer to the overall change from the summed energies of the relaxed clean surface and the respective gas-phase molecule (i.e., $X_{2(g)} \rightarrow 2X_{(a)}$; $X = \mathrm{N}, \mathrm{O}$) or atom (for carbon). Values in bold indicate the lowest-energy site. Dashed values indicate highly unstable sites, where convergence was not obtained.

	Adsorbate					
	C		N		O	
Site	0.5 ML	1.0 ML	0.5 ML	1.0 ML	0.5 ML	1.0 ML
TP	−5.90	–	–	+3.33	–	−1.18
SB	−7.12	−6.69	−0.04	+1.15	−4.78	−3.48
LB	**−8.44**	−8.04	**−1.82**	**−1.23**	−4.48	−4.21
3F	–	**−8.44**	−0.60	–	**−4.90**	−3.81
4F	−7.82	−8.38	–	+0.39	−3.96	**−4.45**

TABLE X. Adsorption energies (eV) on the fcc Ni{110} surface. All adsorption energies refer to the overall change from the summed energies of the relaxed clean surface and the respective gas-phase molecule (i.e., $X_{2(g)} \rightarrow 2X_{(a)}$; $X = \mathrm{N}, \mathrm{O}$) or atom (for carbon). Values in bold indicate the lowest-energy site. Dashed values indicate highly unstable sites, where convergence was not obtained.

	Adsorbate					
	C		N		O	
Site	0.5 ML	1.0 ML	0.5 ML	1.0 ML	0.5 ML	1.0 ML
TP	–	–	+3.94	**−0.96**	−1.46	−0.44
SB	−7.11	−7.68	+0.46	+2.28	−4.04	−2.64
LB	**−8.29**	−7.88	**−1.48**	−0.89	−3.82	**−3.54**
3F	−7.97	−8.46	−0.58	−0.06	**−4.14**	−3.44
4F	−7.91	**−8.47**	−0.58	−0.06	−3.30	−2.84

TABLE XI. Structural characteristics upon adsorption on the fcc Fe{110} surface. δ_{12} and δ_{23} are the distances (normal to the surface) between layers 1 (the surface layer) and 2 and between layers 2 and 3, respectively. Distances are expressed as both an absolute value (Å) and a percentage change relative to the equivalent distance in the clean surface. X-S and X-(S-1) are the distances between the adsorbate and the nearest surface and subsurface atoms, respectively. d_z is the distance between the adsorbate and the plane of the top-layer surface atoms.

			δ_{12}		δ_{23}		Distance (Å)		
X	θ	Site	(Å)	(%)	(Å)	(%)	X-S	X-(S-1)	d_z (Å)
C	0.5 ML	LB	1.09	−4.81	1.35	−1.40	1.81	1.92	0.33
C	1.0 ML	LB	1.18	+3.66	1.29	−5.32	1.82	1.92	0.25
N	0.5 ML	LB	1.09	−4.41	1.34	−2.02	1.80	1.87	0.26
N	1.0 ML	LB	1.18	+3.28	1.28	−5.91	1.81	1.87	0.19
O	0.5 ML	3F	1.16	+1.63	1.32	−3.04	1.83	2.04	0.77
O	1.0 ML	4F	1.14	−0.21	1.34	−1.79	1.79	1.92	0.64

TABLE XII. Structural characteristics upon adsorption on the fcc Co{110} surface. δ_{12} and δ_{23} are the distances (normal to the surface) between layers 1 (the surface layer) and 2 and between layers 2 and 3, respectively. Distances are expressed as both an absolute value (Å) and a percentage change relative to the equivalent distance in the clean surface. X-S and X-(S-1) are the distances between the adsorbate and the nearest surface and subsurface atoms, respectively. d_z is the distance between the adsorbate and the plane of the top-layer surface atoms.

			δ_{12}		δ_{23}		Distance (Å)		
X	θ	Site	(Å)	(%)	(Å)	(%)	X-S	X-(S-1)	d_z (Å)
C	0.5 ML	LB	1.15	+4.96	1.31	−0.06	1.80	1.98	0.33
C	1.0 ML	3F	1.64	+49.79	1.20	−8.35	1.93	2.06	0.07
N	0.5 ML	LB	1.21	+10.10	1.30	−0.90	1.78	1.94	0.24
N	1.0 ML	LB	1.38	+25.97	1.26	−3.97	1.78	1.91	0.05
O	0.5 ML	3F	1.15	+4.95	1.29	−1.17	1.85	2.08	0.83
O	1.0 ML	4F	1.30	+18.61	1.23	−5.74	1.84	1.95	0.56

TABLE XIII. Structural characteristics upon adsorption on the fcc Ni{110} surface. δ_{12} and δ_{23} are the distances (normal to the surface) between layers 1 (the surface layer) and 2 and between layers 2 and 3, respectively. Distances are expressed as both an absolute value (Å) and a percentage change relative to the equivalent distance in the clean surface. X-S and X-(S-1) are the distances between the adsorbate and the nearest surface and subsurface atoms, respectively. d_z is the distance between the adsorbate and the plane of the top-layer surface atoms.

			δ_{12}		δ_{23}		Distance (Å)		
X	θ	Site	(Å)	(%)	(Å)	(%)	X-S	X-(S-1)	d_z (Å)
C	0.5 ML	LB	1.16	+1.09	1.33	+3.49	1.79	1.92	0.25
C	1.0 ML	4F	1.84	+60.30	1.23	−4.26	1.89	1.97	0.00
N	0.5 ML	LB	1.31	+13.79	1.32	+1.97	1.77	1.88	0.07
N	1.0 ML	TP	1.24	+8.47	1.23	−4.34	1.87	–	1.74
O	0.5 ML	3F	1.18	+2.66	1.29	+0.24	1.83	1.98	1.71
O	1.0 ML	LB	1.53	+33.52	1.27	−1.85	1.77	2.04	0.07

effectively unaltered. The substantial changes seen in the expansion and contraction of the layers must, therefore, be related to a significant electronic effect that is not resultant from any geometrical alteration. Oxygen causes an expansion (∼0.02 Å) between the surface and the first subsurface layer at low coverage and appears to have little effect between the same at higher coverage. Also, contrary to the carbon and nitrogen examples, oxygen incurs the greater contraction between the second and third iron layers at low coverage (∼0.04 Å) and a smaller contraction at higher coverage (∼0.02 Å). Oxygen does, however, change adsorption site as the fractional coverage is increased, and so these differences in layer distance are likely to be caused (at least in part) by this change in adsorption geometry.

Adsorption of all three elements, regardless of adsorption site and coverage, causes a contraction between the second and third subsurface iron layers. All three also exhibit similar bond lengths (∼1.8 Å) to the surface (at both high and low coverage), implying a similar strength of bond.

Cobalt, as noted earlier in this paper, readily expands the gap between surface and first subsurface layers upon adsorption of a wide variety of elements, including carbon, nitrogen, and oxygen. Unlike iron, however, the magnitude of the effect that carbon and nitrogen induce is different between the two adsorbates, with nitrogen causing a greater perturbation. In seeming indifference to the various structural alterations that the adsorbates induce, both carbon and nitrogen have a bond length to the nearest metal atom of ∼1.8 Å, as was the case with iron. Oxygen, again moving from the threefold hollow position to the fourfold hollow as we increase the coverage, results in much greater expansions and contractions (δ_{12} and δ_{23}, respectively) than were observed with iron.

Moving on to the nickel surface, and as we saw in the case of cobalt, all three adsorbates induce an expansion between the uppermost layers of fcc Ni{110}; however, there is no universal shrinking between the second and third layers, as we saw in the iron and cobalt examples. Instead, we see some expansion in δ_{23} at a low coverage of all adsorbates, but at the higher, 1.0 ML, coverage we again find that each of the adsorbates cause a contraction in the second and third layers, as before. For adsorption in all of the long-bridge sites we note that the bond length remains similar to that seen previously, with cobalt and iron (∼1.8 Å). A longer bond length is observed for the atop 1.0 ML nitrogen coverage, perhaps implying a weaker overlap between the nitrogen and nickel orbitals. Zhang and Tang[55] have previously studied the adsorption of oxygen on a similar Ni{110} surface. Upon the adsorption of 0.5 ML O, they reported an expansion of the first interlayer spacing (δ_{12}), while finding a small contraction of the second interlayer spacing (δ_{23}). This is in broad agreement with our results, where we, too, have an expansion of δ_{12}; however, we find that δ_{23} also has a slight expansion. This difference may be attributed to the different adsorption sites found to be the most stable (SB for Zhang and Tang, 3F for us)

TABLE XIV. Charges (in e) retained by the adsorbate (Ads) and the first and second surface Fe{110} layers [S and (S-1), respectively] for each adsorbate. Values are averaged over all of the atoms in the layer.

		Clean	Carbon	Nitrogen	Oxygen
	Ads	–	−1.02	−1.18	−0.98
0.5 ML	S	0.03	0.32	0.35	0.36
	S-1	−0.03	0.17	0.17	0.09
	Ads	–	−0.86	−1.07	−0.98
1.0 ML	S	0.03	0.52	0.64	0.67
	S-1	−0.03	0.24	0.33	0.27

TABLE XV. Charges (in e) retained by the adsorbate (Ads) and the first and second surface Co{110} layers [S and (S-1), respectively] for each adsorbate. Values are averaged over all of the atoms in the layer.

		Clean	Carbon	Nitrogen	Oxygen
	Ads	–	−0.85	−1.10	−1.01
0.5 ML	S	0.01	0.28	0.33	0.36
	S-1	−0.03	0.12	0.18	0.11
	Ads	–	−0.72	−0.97	−0.98
1.0 ML	S	0.01	0.42	0.57	0.70
	S-1	−0.03	0.24	0.39	0.24

TABLE XVI. Charges (in e) retained by the adsorbate (Ads) and the first and second surface Ni{110} layers [S and (S-1), respectively] for each adsorbate. Values are averaged over all of the atoms in the layer.

		Clean	Carbon	Nitrogen	Oxygen
	Ads	–	−0.74	−1.01	−0.95
0.5 ML	S	0.00	0.23	0.32	0.33
	S-1	−0.01	0.12	0.18	0.11
	Ads	–	−0.64	−0.24	−0.92
1.0 ML	S	0.00	0.43	0.21	0.61
	S-1	−0.01	0.21	0.02	0.34

TABLE XVII. Spin moments (in μ_B) retained by the adsorbate (Ads) and the first and second surface Fe{110} layers [S and (S-1), respectively] for each adsorbate. Values are averaged over all of the atoms in the layer.

		Clean	Carbon	Nitrogen	Oxygen
	Ads	–	−0.20	−0.09	0.13
0.5 ML	S	2.95	2.28	2.27	2.54
	S-1	2.47	1.80	1.60	2.46
	Ads	–	−0.22	−0.12	0.05
1.0 ML	S	2.95	1.60	1.75	1.66
	S-1	2.47	0.98	0.84	2.23

TABLE XIX. Spin moments (in μ_B) retained by the adsorbate (Ads) and the first and second surface Ni{110} layers [S and (S-1), respectively] for each adsorbate. Values are averaged over all of the atoms in the layer.

		Clean	Carbon	Nitrogen	Oxygen
	Ads	–	−0.01	0.00	0.21
0.5 ML	S	0.74	0.35	0.33	0.67
	S-1	0.62	0.23	0.34	0.63
	Ads	–	0.00	−0.03	0.20
1.0 ML	S	0.74	0.01	0.38	0.38
	S-1	0.62	0.06	0.63	0.66

and the different GGA functional used (PBE for Zhang and Tang, PW91 for us).

2. *Electronic and magnetic properties*

The atomically resolved charges that are resultant in each of these systems are tabulated for iron (Table XIV), cobalt (Table XV), and nickel (Table XVI). The values of the charge for each of the adsorbate systems (with the exception of 1.0 ML carbon) on iron and cobalt can be directly compared as adsorption on these structures occurs in the same location. Indeed, these adsorption sites also remain favorable for 0.5 ML coverage on the nickel surface. There is, for each surface, a substantial negative charge that is transferred to each adsorbate, as has been observed on other, similar, systems.[34] In each case, nitrogen develops the greatest charge, not oxygen, as we would have expected from merely considering conventional electronegativities.

Regardless of the surface, adsorption of 0.5 ML of any of these adsorbates results in a surface-layer charge of $+0.3e$ $0.4e$ per metal atom, and if the adsorption geometries remain unaltered as we increase the coverage to 1.0 ML, then the charge on this surface layer increases to $+0.4e$–$0.7e$ per metal atom. Conversely, increasing the coverage results in a general *decrease* in the quantity of charge acquired by each adsorbate atom (this depolarisation presumably caused by electrostatic repulsion between adatoms). In all cases the subsurface layer (S-1) is positively charged also, with the electrostatic repulsion between the two metallic layers likely to be a strong contributor to their expansion.

TABLE XVIII. Spin moments (in μ_B) retained by the adsorbate (Ads) and the first and second surface Co{110} layers [S and (S-1), respectively] for each adsorbate. Values are averaged over all of the atoms in the layer.

		Clean	Carbon	Nitrogen	Oxygen
	Ads	–	−0.15	−0.02	0.26
0.5 ML	S	1.86	1.34	1.41	1.88
	S-1	1.63	1.31	1.50	1.75
	Ads	–	−0.13	−0.05	0.20
1.0 ML	S	1.86	0.60	0.66	1.68
	S-1	1.63	0.83	1.11	1.65

There are several trends present in the spin moments that result from the adsorption of each species on these surfaces. Oxygen, for example, generally retains a moderate moment ($0.1\mu_B$–$0.3\mu_B$) and always couples ferromagnetically, irrespective of whether it adsorbs on iron (Table XVII), cobalt (Table XVIII), or nickel (Table XIX). Similarly, carbon retains a moment up to $\sim 0.2\mu_B$ and always couples antiferromagnetically to the surface. Last, nitrogen appears to only retain a weak moment (up to $\sim 0.1\mu_B$) and also couples antiferromagnetically to the surface.

Carbon or nitrogen at 0.5 ML on the surface results in a substantial suppression of the surface-layer magnetic moment (Fig. 7). For iron, there is a ∼24% decrease compared to the clean {110} surface; with cobalt this suppression varies between 24% and 28%, and for nickel there is a much larger 53%–55% drop. The effect of 0.5 ML adsorption on the subsurface layer is not as neatly segregated, but both carbon and nitrogen still induce a suppression in this layer, with a magnitude varying between 27% and 35% for iron, 8% and 20% for cobalt, and 45% and 63% for nickel. There is a general, concave, trend (in Fig. 7) for each of these adsorbates as we run from iron to cobalt to nickel. We can also conclude that carbon and nitrogen always have similar effects on the spin

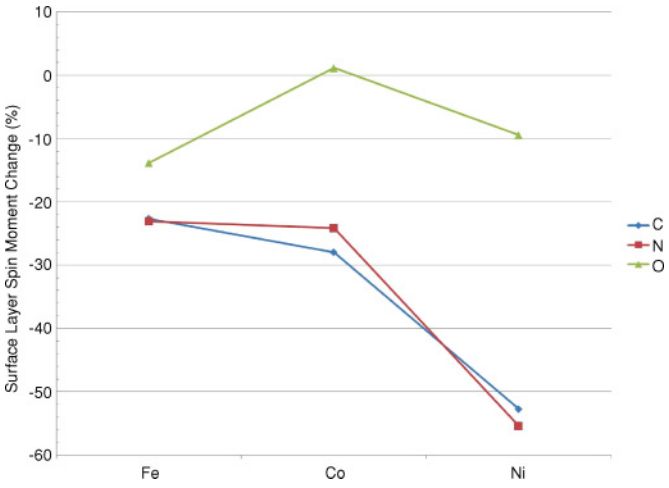

FIG. 7. (Color online) Effect of 0.5 ML of carbon, oxygen, and nitrogen on the surface spin magnetic moment of iron, cobalt, and nickel fcc {110} surfaces, expressed as a percentage change over the clean-surface value.

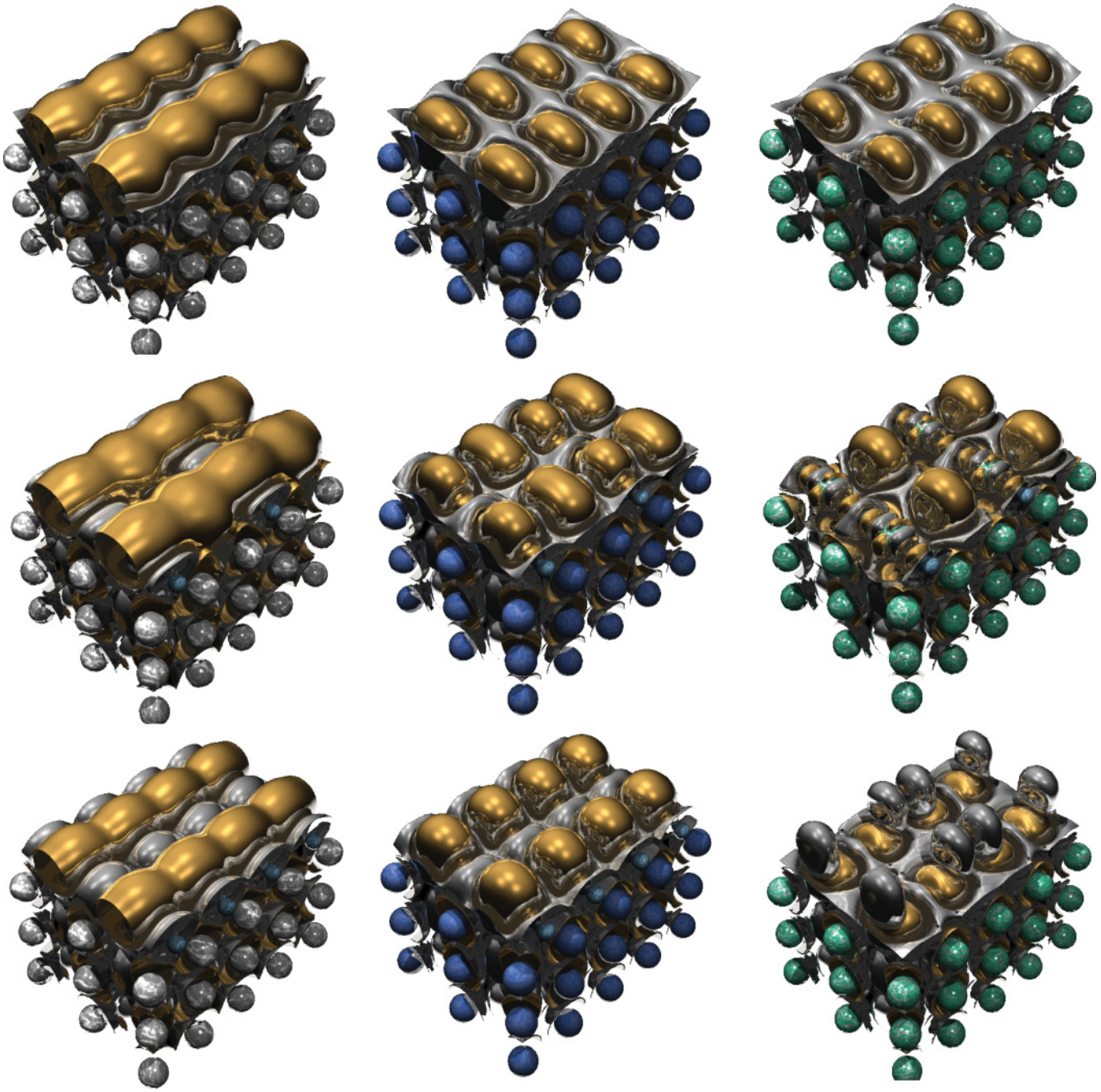

FIG. 8. (Color online) Isosurfaces of residual spin density ($\rho_\alpha - \rho_\beta$) for the clean iron, cobalt, and nickel {110} surfaces (top row) and for their equivalent 0.5 ML N-adsorbed surfaces (middle row) and 1.0 ML adsorbed surfaces (bottom row). Gray spheres represent iron, dark blue represent cobalt, and green represent nickel. The smaller light-blue spheres (where visible) represent nitrogen. Gold and silver represent net majority and minority spin, respectively, at a level of $1 \times 10^{-3} \mu_B$ Å^{-3}.

magnetic moment of each of these surfaces, and both exhibit a larger effect than that of oxygen.

A visual representation of the impact of 0.5 ML of nitrogen on the residual majority and minority spin of each of these surfaces is shown in Fig. 8. In these three systems, nitrogen adsorption is most stable in the long-bridge position, so the relative effects between each surface can be easily compared. The most striking effect occurs with adsorption on nickel, with the residual majority spin on the surface nickel atoms closest to the nitrogen adatoms being very strongly reduced. The residual majority spin for the other surface nickel atoms appears to be slightly enhanced with respect to the clean surface. This results in an overall decrease in the average surface-layer moment, although there are still areas on the surface with moments of notable magnitude.

Oxygen, at 0.5 ML, reduces the moment of the surface layer between 9% and 14% for nickel and iron and leaves the surface moment for cobalt unchanged. For the subsurface layer, the

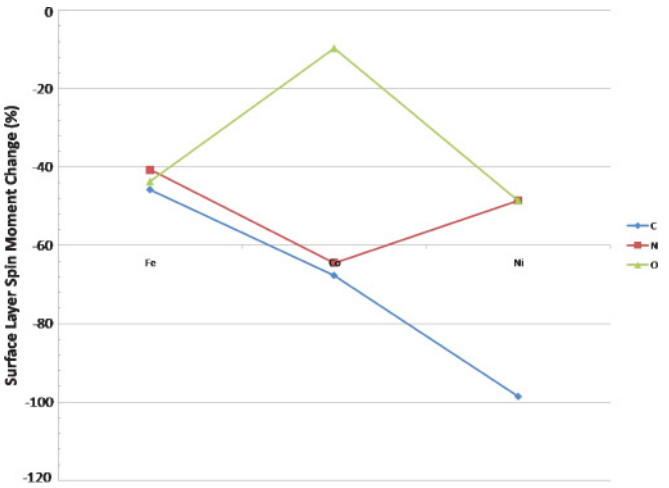

FIG. 9. (Color online) Effect of 1.0 ML of carbon, oxygen, and nitrogen on the surface spin magnetic moment of iron, cobalt, and nickel fcc {110} surfaces, expressed as a percentage change over the clean-surface value.

moment is unchanged in the case of iron, and *enhanced* by 2%–7% for nickel and cobalt. These results are in excellent agreement with the work on oxygen adsorption on Ni{110} by Zhang and Tang.[55] They report clean nickel surface and subsurface moments of $0.74\mu_B$ and $0.63\mu_B$, respectively. Upon oxygen adsorption, they find the moment retained by the adsorbate is $0.21\mu_B$ and ferromagnetically coupled to the surface, while the surface and subsurface moments remain relatively unchanged.

As we move to higher coverage, the suppressive effect of carbon and nitrogen on the surface moment becomes much greater (in the instances where the adsorption location remains unchanged). In the case of iron, the surface-layer moment is lower by ∼41%–46%, for cobalt a substantially larger decrease of 65%–68% is observed, and for nickel an immense 99% drop in the surface-layer moment is seen upon 1.0 ML carbon adsorption (Fig. 9). Oxygen, too, has a stronger influence at this higher coverage, suppressing the surface moment of iron by around 44%, that of cobalt by ∼10%, and that of nickel by around 49%. The general trend (in Fig. 9) for oxygen and carbon is, once again, roughly concave as we run from iron to cobalt to nickel. However, the trend for nitrogen is now convex across the three surfaces. This is caused by the slightly anomalous result at 1.0 ML nitrogen coverage on a nickel surface, where we have spontaneous molecular N_2 formation. We further conclude that, at this higher coverage, the effect of nitrogen and carbon on each of these surfaces are, again, of roughly similar intensity and always greater than that of oxygen (excepting the case of Ni{110}/N).

A visual representation of the impact of 1.0 ML of nitrogen on the residual majority and minority spin of each of these surfaces is shown in Fig. 8.

We can see from Fig. 8 that 1.0 ML of nitrogen adatoms on a nickel surface results in the formation of N_2. This formation, however, is only preferred over the long-bridge position (with no molecular arrangement) by a scant 0.07 eV. In order to ascertain whether the molecular arrangement seen in the case of nickel is also lower in energy for the other FM surfaces, further calculations were performed that used the final geometry of the nickel calcuation as the starting geometries for the cobalt and iron surfaces. It was found, after these surfaces and adsorbates were allowed to relax, that molecular nitrogen formation is not the lowest-energy solution for either the iron or the cobalt surfaces. In the case of iron, formation of N_2 resulted in a system that was ∼2 eV less stable than the long-bridge arrangement seen in Fig. 8. For cobalt, the difference in energy was ∼0.5 eV.

The spin moments retained by the subsurface layers are equally quashed by the greater coverage of carbon and nitrogen with values lowered by approximately 60%–66% for the iron systems, 32%–49% for cobalt, and again an astonishingly large 90% for carbon adsorbed on nickel. Oxygen adsorption now also results in a lower spin moment for the subsurface layer in iron, with a 10% drop in value. Similar adsorption on cobalt and nickel, however, still induces an enhancement of the subsurface moment, albeit only marginally (∼1%).

The partial densities of states focusing on the surface layer of the metal are shown in Fig. 10 for the carbon-adsorbed surfaces, Appendix B for nitrogen and Appendix C (see Ref. 54) for the oxygen-adsorbed surfaces. The major effect of adsorption that occurs on all of these metal surfaces is a general flattening of the surface *d*-state peak, spreading out both to higher and lower energies, caused by overlap with the various adsorbate *p* states. This flattening is far more noticeable for the majority states than for minority states, and especially with higher coverages of adsorbates.

In the case of the carbon-adsorbed surfaces (Fig. 10), we can see that the adsorbate *s* and *p* states remain in roughly the same location on each of the FM surfaces, and with a similar degree of broadening (with respect to the surface coverage). Comparing the low and high coverage systems on each of these surfaces, we can see the greater degree of *p*-state broadening that occurs at greater coverage of carbon, with a corresponding broadening of the surface-layer *d* states at equivalent energies.

With the exception of 1.0 ML coverage on nickel, the nitrogen-adsorbed systems (Appendix B; see Ref. 54) all have adsorbate *s* and *p* states in approximately the same location, and again with a similar degree of broadening. For 1.0 ML of nitrogen on nickel, we have molecular N_2 spontaneously forming on the surface, and this can be seen in the PDOS plots where we have adsorbate *s* and *p* states that shift, split, and mix to form molecular orbitals. At this coverage of nitrogen, the surface-layer nickel *d* states are similarly narrower than at lower coverage.

The oxygen *s* and *p* states, when adsorbed on iron cobalt and nickel (Appendix C; see Ref. 54), are, once again, at approximately the same energies across the surfaces. What is interesting, however, is that the spin splitting of the adsorbate *s* and *p* orbitals is noticeably smaller when adsorbed on iron, than for equivalent adsorption on either cobalt or nickel. We can again see that there is an increased broadening of the adsorbate *p* states as we move from a low to a high coverage, with the coupled broadening of surface-layer *d* states at these energies.

Adsorption of 0.5 ML of carbon and nitrogen on each of these surfaces occurs in a relatively asymmetric location—the long-bridge site. This results in two very different

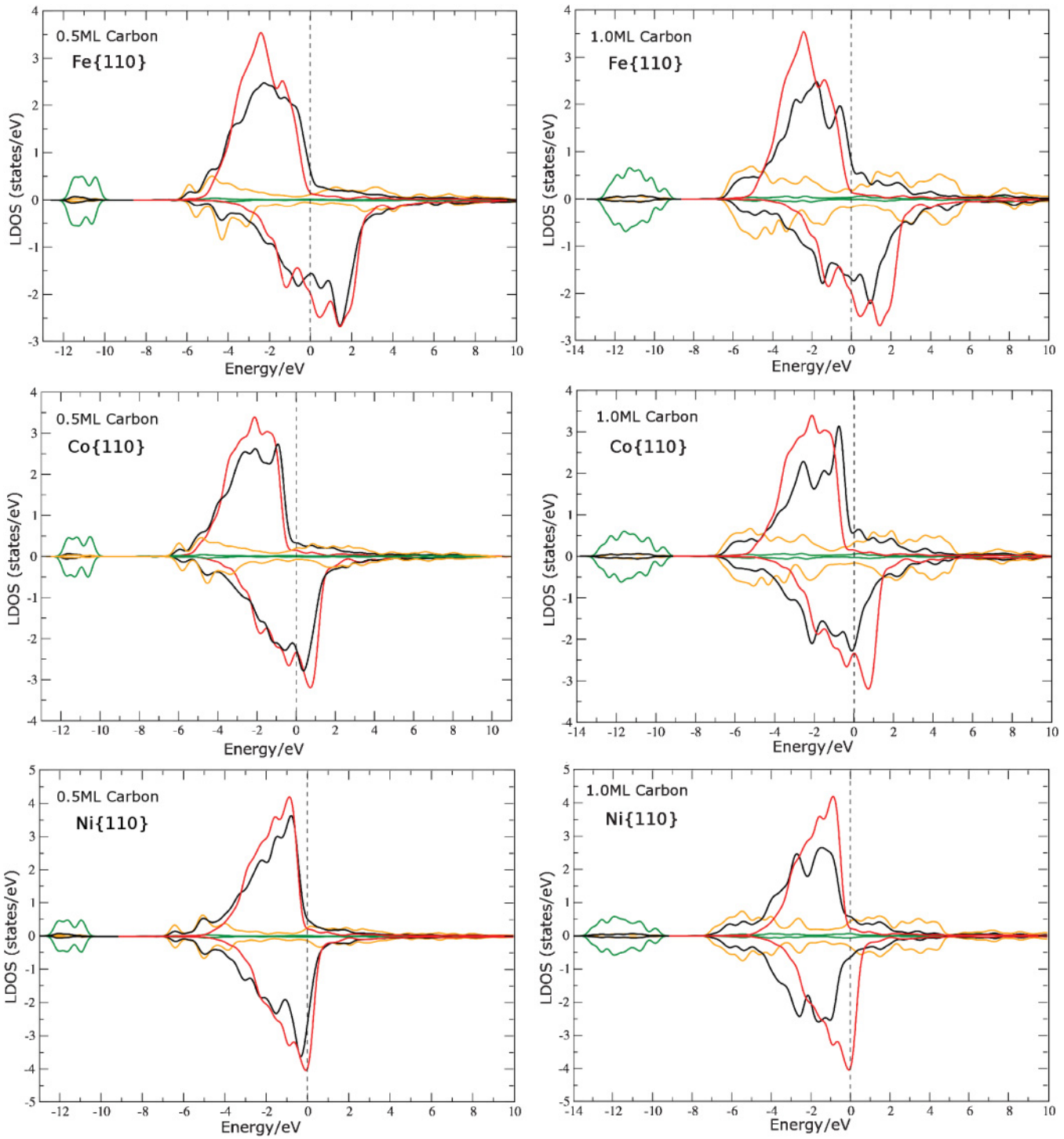

FIG. 10. (Color online) Spin-resolved projected DOS for the surface layer of various carbon-metal{110} systems at both 0.5 and 1.0 ML coverage, with majority (minority) states on the upper (lower) half of each plot. The average metal surface-layer *d* states for the clean surface are shown in red, with the average metal surface-layer *d* states for the adsorbed surface shown in black. Adsorbate *p* states (orange) and *s* states (green) are also illustrated. The Fermi level is set at 0 eV.

environments for the surface metal atoms. To help analyze the extent of the influence of the adsorbate, separate surface partial DOS plots have been created and are shown in Fig. 11. In these graphs, we have separated the *d* states arising from the two surface atoms and we can see that the adsorbate has a particularly localized effect on the metal states. We can see that it is only the states that arise from the nearest metal atom that overlap strongly with the adsorbate *p* states and that those emanating from the other surface atom remain generally close to those seen for the clean surface. It is interesting to note

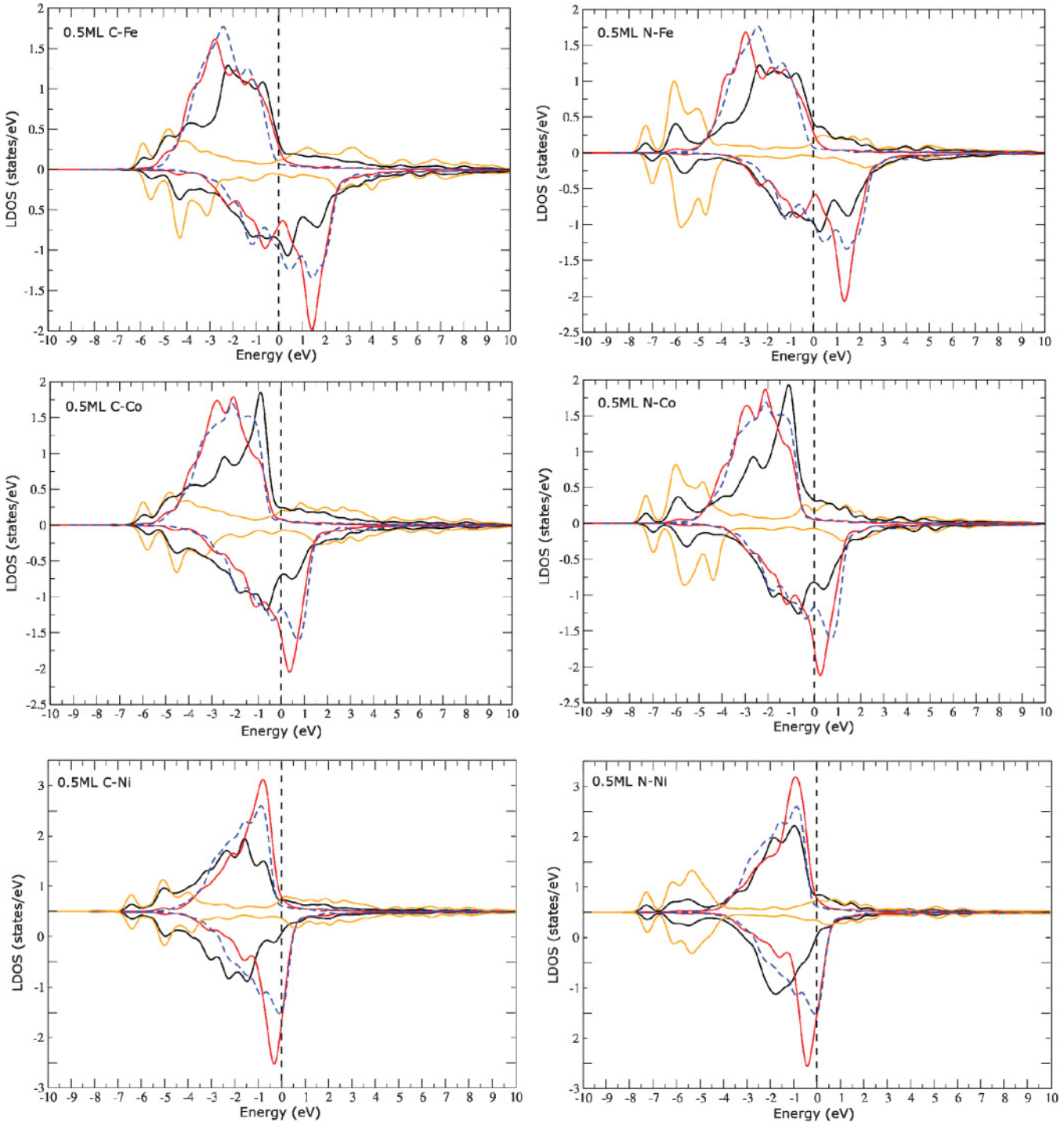

FIG. 11. (Color online) Spin-resolved local DOS for the surface layer of 0.5 ML C/N-metal{110} systems. The clean metal surface-layer *d* states are illustrated by a dashed blue line, the metal *d* states for the surface atom closest to the adsorbate shown in black, and those for the other surface metal atom in red. Adsorbate *p* states (orange) are also shown. The Fermi level is set at 0 eV.

that, for all combinations of surface and adsorbate, there is a distinct enhancement of the intensity of one of the peaks in the minority spin that is close to the Fermi level. In all cases these states are located on the surface metal atom that is further away from the adsorbate, with the heightened intensity attributed to shifted states that were originally at a lower energy in the minority-spin regime. This phenomenon also occurs for the majority spin in nickel (with either carbon or nitrogen adsorbate), with the apex of the peak located just below the Fermi level.

IV. CONCLUSIONS

A. Adsorbate trends

In this paper, we have investigated the influence that several simple atomic adsorbates exert on an fcc cobalt surface. We have seen that all of the adsorbates affect the physical structure of the surface in a qualitatively similar way; they each expand the distance between the top two surface layers, and contract that of the next two layers, with respect to the clean Co{110} surface. Moving from this gross structural change to a more subtle electronic one, we have found that each of these adsorbates results in a distinct shift in the density of *d*-states of the Co surface and have highlighted the correlation between the relative occupancy of the minority and majority *d* states and the spin moment retained by the surface layer.

We looked at the atomically resolved charge transfer and spin moments and we found that there was no clear correlation between the charge transfer and the change in spin moments observed for our systems. The positive charging of the surface would become more significant and contribute more to the spin moment of the surface, as the quantity of adsorbate increases.[56]

The adsorbates were found to couple both ferro- and antiferromagnetically to the surface, with neither the direction (AF or FM) nor the magnitude of the spin moment retained by the adsorbate a clear indicator of the surface-layer moment value. However, there is a distinct trend across the first row of the *p*-block elements to move from AF coupling (on the left, with boron) to FM (at fluorine), with a peak in the FM magnitude occurring at oxygen. Increasing the surface coverage generally resulted in a decrease in the surface spin moment, with the exception of fluorine, where a moderate enhancement ($\sim$11%) of the surface moment occurs at 1.0 ML coverage.

B. Substrate trends

In addition to studying trends across the periodic table for adsorbates, we have also investigated trends for different substrates by examining the similarities and differences found between the adsorption of oxygen, carbon, and nitrogen atoms on fcc iron, cobalt, and nickel surfaces. We have found that there is a general propensity for C and N to adsorb in relatively low coordinated sites (e.g., bridge), especially at low coverage. Oxygen retains its preference for higher coordinated hollow positions, as we have seen earlier in the case of cobalt.

Several structural trends have been identified—both across the range of adsorbates and across the range of surfaces. For example, adsorption of any of the three species on the Fe{110} surface resulted in a contraction between the second and third layers. Similarly, adsorption of small quantities of oxygen results in a universal expansion of the top two layers of each of these metals.

With regard to electronic effects, adsorption on all of these surfaces resulted in a negatively charged adatom and positively charged surface and subsurface layers. The magnitude of the charge retained by the metal was found to generally increase with adsorbate coverage, while that retained by individual adatoms decreases (however, the amount retained by the adsorbate layer, as a whole, naturally increases).

Magnetically, carbon, nitrogen, and oxygen all greatly influence the metal surfaces. Carbon and nitrogen both couple antiferromagnetically to all of the surfaces, while oxygen couples ferromagnetically. The iron surface exhibits the highest magnitude of adatom spin moment, if AF coupled, and the lowest magnitude if the coupling is FM. Both carbon and nitrogen adsorption result in significant suppression of the metallic spin moments, as does oxygen to a lesser extent, with the effect magnified at higher coverage.

Analysis of the partial densities of states, in the case of 0.5 ML carbon and nitrogen adsorption, led to the observation that the influence of the adsorbates was strongly localized, with the surface metal atom nearest to the adsorbate possessing a substantially distorted *d* band compared to the clean surface. The surface atom that is further away has a far less distorted *d* band generally, but does exhibit enhanced peaks in the minority-spin DOS both above (for Co and Fe) and below (for Ni) the Fermi energy.

We have, in this paper, delved into the intricate nature of the bonding between an adsorbate and a FM surface. What we found is that there is a particularly complex relationship between the DOS and the physical and electronic characteristics of the surface. Trends and correlations have been teased from this elaborate mesh of properties, and these form the building blocks of our understanding of these systems.

ACKNOWLEDGMENTS

D.S.D.G. would like to thank the EPSRC for a graduate studentship. S.J.J. is grateful to The Royal Society for a University Research Fellowship. Computational resources were provided by the Cambridge High-Performance Computing Service.

[1] R. Chesnutt, J. Appl. Phys. **73**, 6223 (1993).
[2] G. Broden, G. Gafner, and H. Bonzel, Surf. Sci. **84**, 295 (1979).
[3] E. Iglesia, Appl. Catal., A **161**, 59 (1997).
[4] D. J. Coulman, J. Wintterlin, R. J. Behm, and G. Ertl, Phys. Rev. Lett. **64**, 1761 (1990).
[5] F. Frechard and R. A. van Santen, Surf. Sci. **407**, 200 (1998).
[6] K. Kern, H. Niehus, A. Schatz, P. Zeppenfeld, J. Goerge, and G. Comsa, Phys. Rev. Lett. **67**, 855 (1991).
[7] S. S. P. Parkin, N. More, and K. P. Roche, Phys. Rev. Lett. **64**, 2304 (1990).
[8] T. Herrmann, K. Ludge, W. Richter, N. Esser, P. Poulopoulos, J. Lindner, and K. Baberschke, Phys. Rev. B **64**, 184424 (2001).
[9] W. Ling, Z. Qiu, O. Takeuchi, D. Ogletree, and M. Salmeron, Phys. Rev. B **63**, 024408 (2000).
[10] C. Tolkes, R. Struck, R. David, P. Zeppenfeld, and G. Comsa, Appl. Phys. Lett. **73**, 1059 (1998).
[11] E. Wimmer, A. J. Freeman, M. Weinert, H. Krakauer, J. R. Hiskes, and A. M. Karo, Phys. Rev. Lett. **48**, 1128 (1982).
[12] S. Hope, E. Gu, M. Tselepi, M. E. Buckley, and J. A. C. Bland, Phys. Rev. B **57**, 7454 (1998).

[13]K. P. Kopper, D. Küpper, R. Reeve, T. Mitrelias, D. S. D. Gunn, and S. J. Jenkins, Phys. Rev. B **80**, 052406 (2009).
[14]D. S. D. Gunn, D. Kupper, S. J. Jenkins, and J. Bland, Surf. Sci. Lett. **603**, L45 (2009).
[15]P. Blonski, A. Kiejna, and J. Hafner, Surf. Sci. **590**, 88 (2005).
[16]S. R. Chubb and W. E. Pickett, Phys. Rev. Lett. **58**, 1248 (1987).
[17]H. Huang and J. Hermanson, Phys. Rev. B **32**, 6312 (1985).
[18]R. Q. Wu and A. J. Freeman, J. Magn. Magn. Mater. **127**, 327 (1993).
[19]S. J. Jenkins, Surf. Sci. **600**, 1431 (2006).
[20]S. Pick, P. Legare, and C. Demangeat, J. Phys. Condens. Matter **20**, 075212 (2008).
[21]S. Pick, P. Legare, and C. Demangeat, Phys. Rev. B **75**, 195446 (2007).
[22]D. C. Sorescu, D. L. Thompson, M. M. Hurley, and C. F. Chabalowsky, Phys. Rev. B **66**, 035416 (2002).
[23]T. Bromfield, D. Curulla Ferre, and J. Niemantsverdriet, Chem. Phys. Chem. **6**, 254 (2005).
[24]C. Huo, J. Ren, Y.-W. Li, J. Wang, and H. Jiao, J. Catal. **249**, 174 (2007).
[25]D. Borthwick, V. Fiorin, S. J. Jenkins, and D. King, Surf. Sci. **602**, 2325 (2008).
[26]X. Gong, R. Raval, and P. Hu, Surf. Sci. **562**, 247 (2004).
[27]S. Pick and H. Dreysse, Surf. Sci. **540**, 389 (2003).
[28]S. Pick and H. Dreysse, Surf. Sci. **474**, 64 (2001).
[29]S. J. Jenkins and D. King, Surf. Sci. **504**, 138 (2002).
[30]S. Pick, Surf. Sci. **601**, 5571 (2007).
[31]W. Clemens, E. Vescovo, T. Kachel, C. Carbone, and W. Eberhardt, Phys. Rev. B **46**, 4198 (1992).
[32]R. Courths, S. Hufner, P. Kemkes, and G. Wiesen, Surf. Sci. **376**, 43 (1997).
[33]J. Hong, R. Q. Wu, J. Lindner, E. Kosubek, and K. Baberschke, Phys. Rev. Lett. **92**, 147202 (2004).
[34]S. Yamagishi, S. J. Jenkins, and D. A. King, Surf. Sci. **543**, 12 (2003).
[35]Q. Ge, S. J. Jenkins, and D. A. King, Chem. Phys. Lett. **327**, 125 (2000).
[36]A. Karmazyn, V. Fiorin, S. Jenkins, and D. King, Surf. Sci. **538**, 171 (2003).
[37]S. J. Jenkins, Q. Ge, and D. A. King, Phys. Rev. B **64**, 012413 (2001).
[38]C. L. Fu and A. J. Freeman, Phys. Rev. B **40**, 5359 (1989).
[39]K. Bird and M. Schlesinger, J. Electrochem. Soc. **142**, L65 (1995).
[40]M. J. Hall, B. J. Hickey, M. A. Howson, M. J. Walker, J. Xu, D. Greig, and N. Wiser, Phys. Rev. B **47**, 12785 (1993).
[41]A report by Shen *et al.* (Ref. 42) shows that fcc Fe can be grown with up to 10 ML thickness (in the {100} orientation) with ferromagnetic surface layers. Although there is some evidence that the ferromagnetism of fcc Fe is lost at greater thicknesses, we have chosen to study the ferromagnetic state of fcc Fe in the present work as we are concerned predominantly with trends in the ferromagnetic metals rather than the details of individual systems.
[42]J. Shen, Z. Gai, and J. Kirschner, Surf. Sci. Rep. **52**, 163 (2004).
[43]S. Clark, M. Segall, C. Pickard, P. Hasnip, M. Probert, K. Refson, and M. Payne, Z. Kristallogr. **220**, 567 (2005).
[44]J. P. Perdew, J. A. Chevary, S. H. Vosko, K. A. Jackson, M. R. Pederson, D. J. Singh, and C. Fiolhais, Phys. Rev. B **46**, 6671 (1992).
[45]D. Vanderbilt, Phys. Rev. B **41**, 7892 (1990).
[46]R. F. W. Bader, *Atoms in Molecules: A Quantum Theory* (Oxford University Press, Oxford, 1990).
[47]These conditions were tested with bulk fcc Co, Ni and Fe with a $6 \times 6 \times 6$ Monkhorst-Pack **k**-point mesh (Ref. 48). The lattice parameters of fcc nickel, cobalt, and iron were found to be 3.541, 3.547, and 3.593 Å, respectively. The bulk magnetic moments were calculated to be $0.62\mu_B$ (Ni), $1.68\mu_B$ (Co), and $2.48\mu_B$ (Fe), all in good agreement with previous experimental (Ref. 49) and theoretical (Refs. 34, 50, and 51) values.
[48]H. J. Monkhorst and J. D. Pack, Phys. Rev. B **13**, 5188 (1976).
[49]R. W. G. Wyckoff, *Crystal Structures*, 2nd ed. (Wiley & Sons, New York, 1963).
[50]M. Alden, S. Mirbt, H. L. Skriver, N. M. Rosengaard, and B. Johansson, Phys. Rev. B **46**, 6303 (1992).
[51]O. Hjortstam, J. Trygg, J. M. Wills, B. Johansson, and O. Eriksson, Phys. Rev. B **53**, 9204 (1996).
[52]We have performed calculations (unpublished) that model the growth of various fcc cobalt orientations {100}, {110}, {111} on top of a copper substrate, up to a thickness of six cobalt monolayers and have found that there is little variation in the magnetic properties of the surface. The surface-layer moment varies from an average of $1.90\mu_B$ for the even layers (2, 4, and 6 ML) to an average of $1.88\mu_B$ for the odd layers (1, 3, and 5 ML). These layers occupy positions very close to their ideal lattice points when added layer by layer, and the band structures of each thickness are very similar, with only a continual addition to bulklike states as the thickness of the cobalt layers is increased. We are therefore confident that adsorption on 6 ML of metal would not give substantially different results for surface properties than adsorption on a greater number of layers.
[53]We have performed calculations with both two and three variable layers. The average spin density using either number of variable layers was found to be $1.74\mu_B$, the maximum difference in atomic position after geometry optimization was found to be ∼0.01 Å, and the difference in total energy between these two systems was found to be <0.001 eV per (1×1) surface unit cell.
[54]See supplemental material at [http://link.aps.org/supplemental/10.1103/PhysRevB.83.115403].
[55]W.-B. Zhang and B.-Y. Tang, Surf. Sci. **603**, 1002 (2009).
[56]D. S. D. Gunn and S. J. Jenkins (unpublished).